Electrical Supporting information

D-tagatose manufacture through bio-oxidation of galactitol derived from waste xylose mother liquor

Feng Sha,[a] Yucong Zheng,[a,b] Jiao Chen,[a] Kequan Chen,[a] Fei Cao,*[a,c] Ming Yan,*[a] and Pingkai Ouyang[a]

Table of contents:

Fig. S1 Summary of major strategies for resourceful utilization of xylose mother liquor. 2

Table S1 Summary of known examples for resourceful utilization of the XML by microorganism fermentation. 3

Fig. S2 Co-production C5&C6 polyols and galactitol from XML by Futaste Co., Ttd. 4

Table S2. GenBank accession numbers of the initial selected candidates by a concise Microbial Protein BLAST search. 5

Fig. S3 Time dependence of the RMSD (Å) of each protein molecule complexed with 1a and NAD(P)$^+$ from MD simulation. 6

Table S3 The detail binding free energies calculated from all-atom molecular dynamic simulations. 7

Table S4 DNA sequences for all genes used in this study. 8

Fig. S4 SDS-PAGE analysis of recombinant biocatalysts. 11

Fig. S5. Michaelis-Menton curve fit of *Pd*PDH with tested substrates (a~g) and *St*NOX with NADH (h). 12

Fig. S6 A binding pose for 1a in modelled *Pd*PDH complexed with NAD$^+$. 13

Fig. S7 Reduced product identification of *St*NOX. 14

Fig. S8 Multiple sequence alignment of *St*NOX to known NADH oxidases. 15

Fig. S9 UV visible absorption spectra of purified *St*NOX 17

Fig. S10 Effect of exogenous flavin cofactor on the activities of recombinant *St*NOX. 18

Fig. S11 Effect of pH and temperature on *Pd*PDH and *St*NOX activity. 19

Fig. S12 HPLC analysis of the stability of NAD$^+$ under reaction condition. 20

Table S5 Effect of metal ions and EDTA on the activity of *Pd*PDH and *St*NOX. 21

Table S6 HPLC analysis conditions for polyols and its corresponding oxidation products. 22

HPLC analysis and spectra 23

^{1}H NMR and ^{13}C NMR spectra 25

References 27

[a] College of Biotechnology and Pharmaceutical Engineering, Nanjing Tech University, Nanjing 211816, China. E-mail: csaofeiw@njtech.edu.cn; yanming@njtech.edu.cn

[b] State Key Laboratory of Bioreactor Engineering, Shanghai Collaborative Innovation Center for Biomanufacturing, East China University of Science and Technology, Shanghai 200237, China

[c] State Key Laboratory of Materials-Oriented Chemical Engineering, Nanjing Tech University, Nanjing 211816, China.

Fig. S1 Summary of major strategies for resourceful utilization of xylose mother liquor.

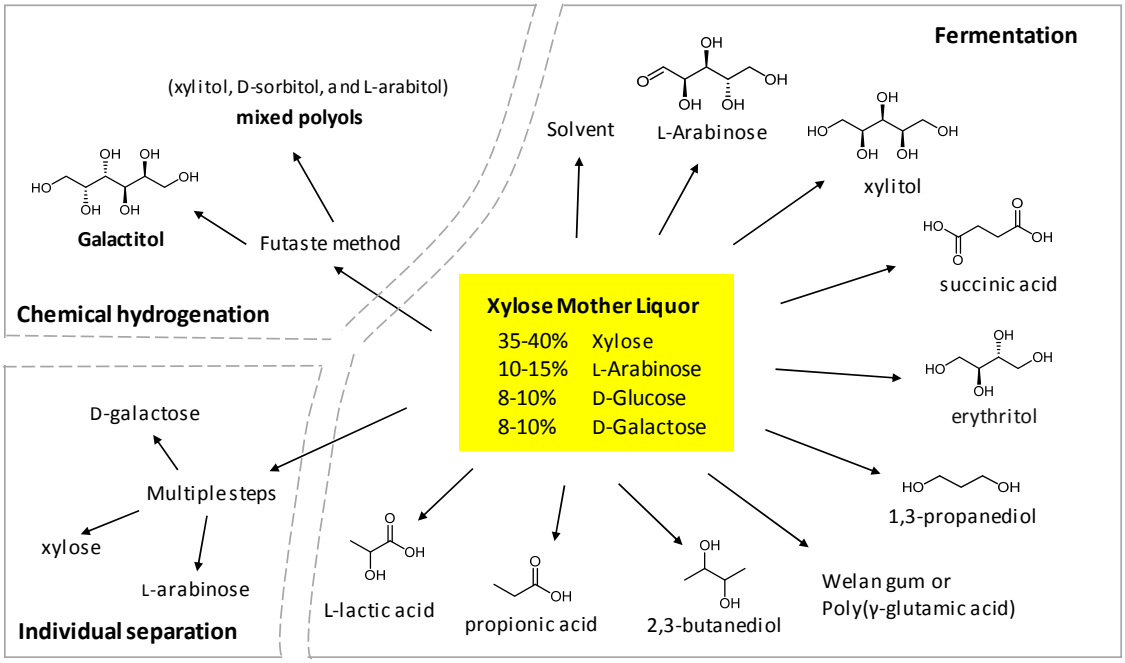

The ways of improving the value of the xylose mother liquor are divided into three major strategies: (A) **Fermentation**, producing useful compounds through microorganism partial utilization /depletion of the sugar mixtures; (B) **Chemical hydrogenation**, hydrogenating the pre-treated XML to polyols mixture by Raney nickel catalyst (**Fig. S2**); (C) **Individual separation**, obtaining xylose, L-arabinose, and D-galactose individually by simulated moving bed chromatography.

Table S1 Summary of known examples for resourceful utilization of the XML by microorganism fermentation.

Organism	Type	Sugar utilization/ depletion	Product	Time [h]	Productivity [g l^{-1} h^{-1}]	Yield [g g^{-1}][a]	Ref.
Bacillus sp. strain	Fed-batch	xylose, glucose, arabinose	L-lactic acid	300	0.38	0.50	1
Klebsiella pneumoniae SDM.	Fed-batch	glucose, arabinose, xylose	2,3-butanediol	61	1.3	0.81	2
Pichia anomala Y161	Batch	glucose, xylose, galactose	L-arabinose	48	N.A.	0.088	3
Bacillus subtilis and *Candida maltosa*	Batch	glucose, arabinose, xylose	xylitol	50	4.25	0.42	4
Propionibacterium acidipropionici	Fed-batch	xylose, glucose, arabinose	propionic acid	256	0.28	N.A.	5
Clostridium acetobutylicum EA 2018	Batch	glucose, xylose, arabinose	solvent	96	0.22	0.33	6
Pichia anomala TIB-x229	Batch	xylose, glucose	sugar alcohols	55	1.08	0.55	7
Escherichia coli	Batch	glucose, xylose, arabinose, galactose	succinic acid	84	0.62	0.63	8
Bacillus subtilis NX-2	Batch	N.A.	poly(γ-glutamic acid)	N.A.	N.A.	0.12	9
Streptomyces hygroscopicus TC03	Fed-batch	glucose, xylose, arabinose,	validamycin A	120	0.11	0.12	10
Aureobasidium pullulans ER35	Batch	glucose, xylose, arabinose	erythritol	144	0.18	0.12	11
Sphingomonas sp. HT-1	Fed-batch	N.A.	welan gum	66	0.34	0.76	12

[a] Product (g)/ total sugar (g).

N.A. not applicable

Fig. S2 Co-production C5&C6 polyols and galactitol from XML by Futaste Co., Ttd..

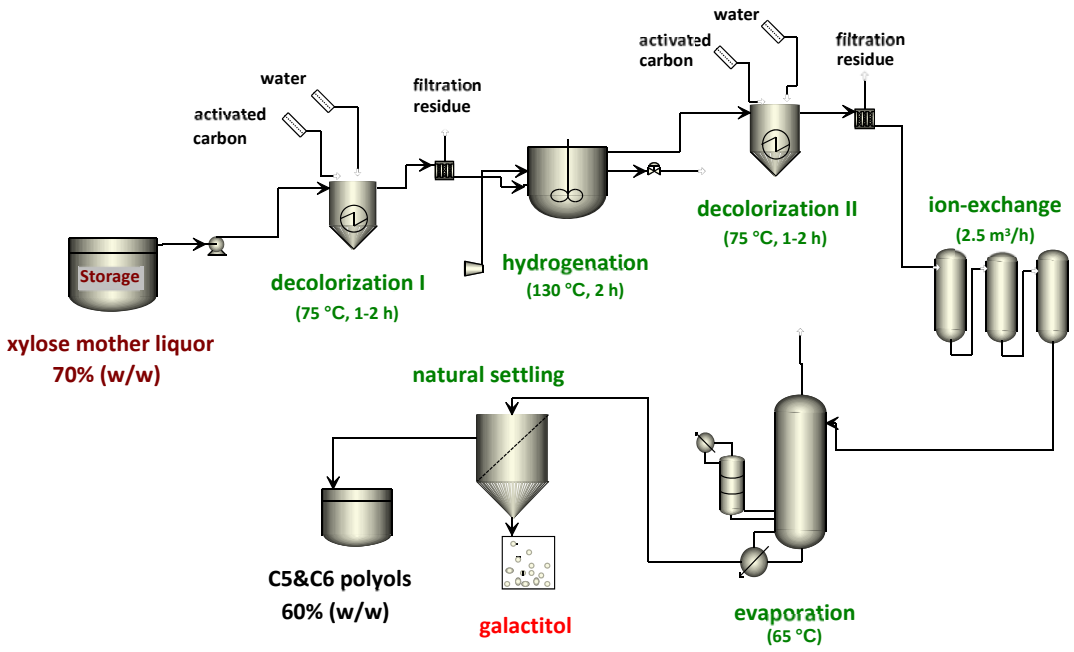

The XML was treated sequentially with the steps of decolorization, hydrogenation, ion exchange and natural sedimentation, from which a clarified solution of C5&C6 polyols and by-product galactitol were obtained (CN Pat., 201010278356.3). In addition, to obtain the administrative license for the use of galactitol, Futaste Co., Ttd. applied for the new food ingredient registry in 2016 at national heath and family planning commission of the People's Republic of China (NHFPC) (http://zwdt.wsjd.gov.cn/).

Table S2. GenBank accession numbers of the initial selected candidates by a concise Microbial Protein BLAST search.

Entry	GenBank accession no.	Entry	GenBank accession no.	Entry	GenBank accession no.	Entry	GenBank accession no.	Entry	GenBank accession no.
1	WP_060857015	26	WP_032720118	51	WP_023941998	76	WP_066568068	101	WP_000768013
2	WP_022595191	27	**WP_005733884**	52	WP_014851288	77	WP_011771040	102	WP_065504365
3	**WP_078308368**	28	WP_055743791	53	WP_100056566	78	WP_096271152	103	WP_084310692
4	WP_076998485	29	WP_040239654	54	WP_021808737	79	WP_010970038	104	WP_008174374
5	~~WP_056572940~~	30	WP_058121638	55	WP_104081300	80	WP_075385615	105	WP_045870196
6	~~WP_026618750~~	31	WP_092009434	56	WP_085670870	81	**WP_011229213**	106	WP_073314389
7	EJM00394	32	WP_035730158	57	WP_015810389	82	WP_061811230	107	WP_010970020
8	WP_073129708	33	WP_042207887	58	WP_011993500	83	WP_101764596	108	KUO70655
9	WP_068166861	34	WP_035150386	59	WP_041975340	84	WP_074256506	109	WP_010967853
10	~~WP_037099020~~	35	WP_068987068	60	WP_011981919	85	OUX81713	110	WP_102879478
11	WP_024926042	36	WP_031409592	61	PIP24785	86	WP_094462405	111	~~WP_044314342~~
12	WP_066150637	37	SLM94108	62	OGV69289	87	WP_002338377	112	OFW58672
13	WP_102888048	38	WP_043303550	63	WP_006542066	88	OGO28466	113	WP_037435435
14	WP_057454804	39	WP_056773817	64	**WP_011751060**	89	WP_022716411	114	OGP87673
15	WP_050774712	40	EHN12801	65	PCH81971	90	CDE26968	115	PIR90072
16	WP_075637083	41	WP_028710629	66	~~WP_016167936~~	91	WP_030090132	116	**KGR09136**
17	~~WP_028752588~~	42	WP_021510787	67	WP_011748444	92	WP_049870661	117	WP_099576466
18	WP_094033569	43	WP_027256047	68	WP_093992377	93	WP_069718745	118	WP_080846483
19	WP_047553035	44	WP_030251078	69	WP_066239482	94	AOT56630	119	PJE69765
20	WP_007700435	45	WP_068441644	70	WP_062271673	95	KMQ76249	120	~~WP_038834460~~
21	WP_066160939	46	WP_023944535	71	WP_011450082	96	WP_024709952	121	WP_026386567
22	WP_055806547	47	WP_076658797	72	EIA13380	97	WP_070299165	122	WP_094613209
23	WP_045165828	48	WP_010192167	73	WP_091582519	98	WP_004625893	123	WP_039296480
24	WP_045028254	49	WP_054374958	74	WP_014695767	99	WP_091494368	124	WP_010283460
25	WP_086659042	50	WP_024845816	75	PIS39375	100	WP_035942099	125	WP_005861942

Redundant sequences were removed with the sequence identity cut-off of 80% (black strikethrough). The final candidates chosen for experimental characterization are highlighted in green.

Fig. S3 Time dependence of the RMSD (Å) of each protein molecule complexed with **1a** and $NAD(P)^+$ from MD simulation.

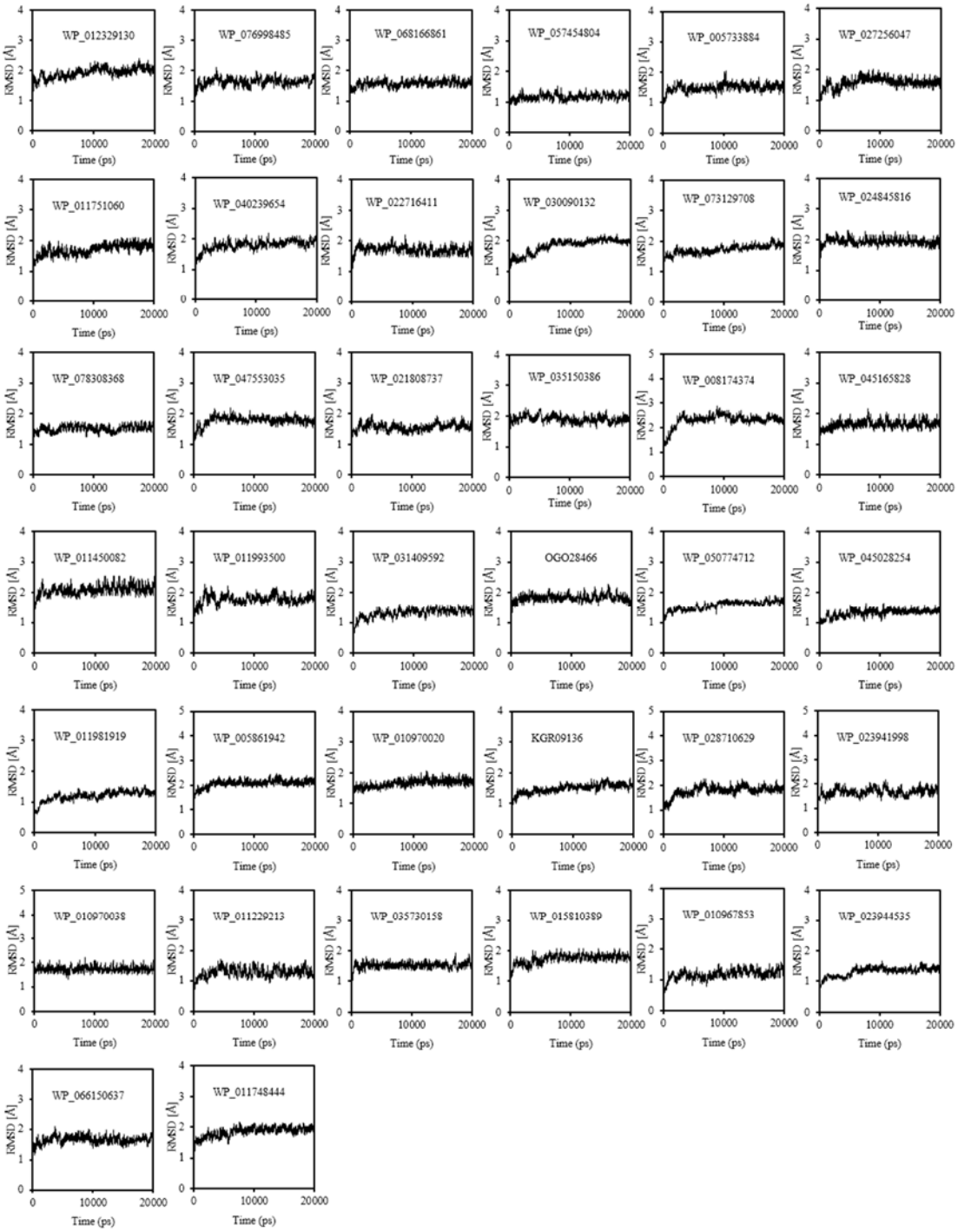

The root mean square positional deviation (RMSD) is the customary parameter to determine the attainment of a stationary state in a simulation of biomolecules. As shown in Fig. S3, the time dependence of the RMSD of each simulation system shows a rather stable trajectory reaching a plateau after 10 ns, thus the MM-PBSA binding free energies were calculated using 1,000 snapshots retrieved from the last 10 ns MD trajectories.

Table S3 The detail binding free energies calculated from all-atom molecular dynamic simulations.

Entry	Enzyme	GenBank accession no.	Amino acid identities with *Psp*PDH [%]	Template PDB code	TM-score[a]	ΔG_{bind} [kcal mol^{-1}]
1	*Psp*PDH	WP_012329130	100	4e6p	1.00	-13.85 ± 2.26
2	*Vp*PDH	WP_076998485	62.79	4e6p	0.98	-13.74 ± 1.52
3	*Ht*PDH	WP_068166861	63.18	1k2w	0.97	-15.63 ± 2.11
4	*Cj*PDH	WP_040239654	60.85	4e6p	0.98	-11.64 ± 2.42
5	*Pd*PDH	WP_011751060	55.47	4e6p	0.98	-16.34 ± 2.01
6	*La*PDH	WP_027256047	53.52	1k2w	0.98	-9.70 ± 1.57
7	*Pss*PDH	WP_057454804	59.77	4e6p	0.99	-14.53 ± 1.87
8	*Ps*PDH	WP_005733884	60.16	4e6p	0.99	-18.34 ±2.72
9	*Rm*PDH	WP_022716411	48.63	1k2w	0.97	-13.40 ± 2.76
10	*Ssp*PDH	WP_030090132	46.83	1k2w	0.96	-11.86 ± 2.53
11	*Ms*PDH	WP_073129708	40.7	3wye	0.93	-10.48 ± 2.81
12	*Pp*PDH	WP_024845816	38.37	3wye	0.93	-14.54 ± 2.65
13	*Ml*PDH	WP_078308368	39.3	3wye	0.94	-17.49 ± 2.23
14	*Sa*PDH	WP_047553035	37.35	1geg	0.93	-14.37 ± 2.71
15	*Lr*PDH	WP_021808737	38.37	3wye	0.95	-13.64 ± 2.25
16	*Gf*PDH	WP_023944535	25.83	5jo9	0.85	-6.94 ± 1.07
17	*Hp*PDH	WP_066150637	25.83	5jo9	0.85	-9.77 ± 1.27
18	*Pad*PDH	WP_011748444	27.08	5jo9	0.85	-8.81 ± 1.63
19	*Tt*PDH	WP_011229213	33.33	4yqz	0.85	-13.18 ± 2.17
20	*Dyf*PDH	WP_015810389	27.31	4h15	0.87	-12.19 ± 1.43
21	*Sin*PDH	WP_010967853	24.5	4h15	0.87	-3.45 ± 2.11
22	*Gl*PDH	WP_035730158	28.4	3ai3	0.90	-4.89 ± 1.78
23	*Php*PDH	WP_045028254	41.53	4z9y	0.90	-5.71 ± 1.96
24	*Df*PDH	WP_050774712	31.98	5u9p	0.90	-11.90 ± 2.01
25	*Ca*PDH	KGR09136	30.08	3ctm	0.84	-12.89 ± 2.15
26	*Kr*PDH	WP_011981919	32.11	3awd	0.90	-9.19 ± 1.23
27	*Sm*PDH	WP_010970020	33.06	3awd	0.89	-12.09 ± 1.75
28	*Pap*PDH	WP_028710629	31.15	3awd	0.89	-8.10 ± 2.81
29	*Gj*PDH	WP_023941998	28.51	3awd	0.91	-5.77 ± 1.71
30	*Sim*PDH	WP_010970038	31.05	3awd	0.90	-10.90 ± 1.65
31	*Ss*PDH	WP_005861942	30.12	1vi8	0.88	-12.40 ± 2.42
32	*Fn*PDH	WP_011993500	38.4	4nbu	0.89	-9.94 ± 1.91
33	*Tc*PDH	WP_045165828	36.73	2uvd	0.91	-12.38 ± 2.37
34	*Mh*PDH	WP_011450082	37.55	2uvd	0.91	-9.09 ± 1.36
35	*Cb*PDH	OGO28466	36.44	3ftp	0.90	-4.15 ± 1.99
36	*Csp*PDH	WP_035150386	38.46	2uvd	0.89	-10.66 ± 2.23
37	*Bsp*PDH	WP_008174374	37.2	1iy8	0.90	-11.53 ± 2.35
38	*Gv*PDH	WP_031409592	41.94	4ure	0.90	-10.94 ± 2.77

[a] 0.5 < TM-score < 1.00, in about the same fold

Table S4 DNA sequences for all genes used in this study.

*Rs*PDH (GenBank accession no: WP_002720244)
ATGCGTCTGGATGGAAAAACCGCTCTGATTACCGGCAGCGCGCGTGGCATTGGCCGTGCGTTCGC GGAAGCGTATGTGCGTGAAGGCGCACGTGTGGCGATAGCGGACATAAATCTGGAAGCCGCACGG GCGACAGCGGCGGAAATTGGCCCTGCGGCGTGCGCTATTGGCCTGGATGTGACCGATCAGGCGAG CATTGACCGTTGCGTCGCGGAGCTGCTGGATCGTTGGGGCCGTATAGATATTCTGGTGAATAATGC GGCACTGTTTGATCTGGCGCCGATTGTGGAGATTACCCGTGAAAGCTATGATCGTCTGTTTGCGAT TAATGTGAGCGGCACCCTGTTTATGATGCAAGCGGTGGCTCGGGCAATGATTGCAGGCGGACGTG GCGGCAAGATTATCAATATGGCGAGCCAGGCAGGCCGTCGTGGTGAAGCGCTGGTGGGCGTGTAT TGCGCGACCAAAGCGGCTGTGATTAGCCTGACCCAGAGTGCGGGCCTGAACCTGATCCGTCATGG CATCAATGTGAATGCGATTGCGCCAGGCGTGGTAGACGGCGAACACTGGGATGGCGTGGATGCGA AGTTTGCGGACTATGAAAACCTGCCTCGTGGCGAGAAAAAACGTCAAGTCGGCGCTGCAGTCCCG TTCGGTCGTATGGGTCGTGCGGAAGATTTGACCGGCATGGCGATTTTTCTGGCGACCCCGGAGGC AGATTACATAGTGGCGCAGACCTATAATGTCGATGGCGGGAATTGGATGAGCTGA
*Rl*GDH (GenBank accession no: WP_011650422)
ATGAGTTATCAGCAGAAATTCCGCCTGGATGGCGAACGTGCAGTGGTTACCGGTGGCGGTCGTGC CATTGGCCTGTGTTGTACCGAAGCCCTGGCAGAAGCCGGTGCCGCAGTGGTTGTGATTGAGCGTA GCGAAGCCGATGCAGAACAGGCACTGGCCCTGCGCAATCGTGGCTATGATGTTGAAGTGCGCGTG GGTGATGTGACAGATGCAGCCCGCATGGATGCAATTGCAACCGAACTGGCCGATGGCGGTCGTCC TGCCACCATTCTGGTGAACAATGCAGGTATCGGCCAGAGCGGTATTCCGGCCCAGGATCTGACCG ATGCCGATTGGCTGCGCATGATGGATGTGAACCTGAACGGCGTTTTCTGGTGCAGCCGTGCCTTTG GCCGCAGCATGATCAGTATGAAACGTGGCGCCATCGTGAATCTGGGCAGCATGAGCGGTACCATT TGCAATCGTCCGCAGCCGCAGACCGCCTACAATGTGAGCAAAGCAGCCGTGCATCACCTGACACG CAGCCTGGCAGCCGAATGGGCCCATCATGGTATTCGCGTGAATGCCGTGGCCCCGACATATATCG AAACCCCTATGGTGGTGGCAGTTGAAGCAAATCGCGAACGCATTCCGCTGTGGCTGGCAGATACC CCGATGGCACGCATGGGTACACCGGAAGAAGTGGCAAGTGCCGTTCTGTTTCTGGCCAGCGGTGC AGCCAGCCTGATGACCGGTGCCATTGTGAACGTGGATGCCGGTTTTACCTGCTGGTGA
*Rc*PDH (GenBank accession no: WP_013067749)
ATGCGCCTGACCGGCAAACGTGCCCTGATTACCGGTGCCGCACGTGGCATCGGTCGTGCATTTGC CGAAGCATATCTGCGCGAAGGTGCCGACGTGACCATTGGCGATATTAACCTGGAGGGCGCCCGTA AAACAGCCGCCGAAATTGGTTGCGCCGCCGTTCATCTGGATGTGACCGACCAGGCCAGCATCGAT GCAGCAATGGCCGTTATGCGCGCCGGTGGCGGTATCGACATCCTGATTAACAACGCCGCCATTTTT ACCGCCGCCCCGATCGATGAAATCACCCGCGCCGATTACGATCGCGTGTTTGCCATCAACGTGGC CGGTACCCTGTTCACCCTGCAGGCAGCAGCACGCGAAATGATTGCCCAGGGCCGCGGCGGTAAAA TCATCAACATGGCCAGTCAGGCAGGTCGCCGCGGTGAAAGTCTGGTGGCCGTGTATTGCGCCAGC AAAGCCGCCGTGATTAGCCTGACCCAGAGCGCCGGTCTGAACCTGATTGCCCACGGCATCAATGT GAATGCCATTGCCCCGGGCGTGGTGGATGGTGAACATTGGGATGGCGTGGACGCCTTCTTTGCCA AATACGAGAAAAAGCCGCTGGGCCAGAAGAAAAAAGAAGTTGGCGCAAGCGTTCCGTTTGGCCG CATGGGCACCGCAGCAGACCTGACAGGCATGGCCATTTTTCTGGCCACCCCGGAAGCCGACTATA TTGTGGCCCAGACCTACAATGTTGACGGCGGCAACTGGATGTGA
*Psp*PDH (GenBank accession no: WP_012329130)
ATGCGTCTGGAAGACAAAGTGGCCATTCTGACCGGTGCAGCCAGCGGTATCGGTGAAGCCGTTGC CCAGCGTTATCTGGATGAGGGTGCCCGCTGCGTTCTGGTTGACGTGAAACCGGCCGGTGGTAGTCT

GGCCCGCCTGATTGAAGCAAATCCGGGCCGTGCAGTTGCCGTTACCGCCGATGTGACCCGTCGTG ATGATATCACCCGTATCGTTGCCACCGCAGTTGAGCGCTTTGGCGGCGTGGATATTCTGTTCAACA ACGCCGCACTGTTTGACATGCGTCCGCTGCTGGATGAAAGCTGGGATGTGTTTGACCGCCTGTTCA GCGTGAACGTGAAGGGCCTGTTCTTTCTGATGCAGGCCGTTGCCCAACGTATGGTGGAGCAGGGT CGCGGCGGCAAAATCGTGAATATGAGCAGCCAGGCAGGTCGTCGTGGCGAGGCACTGGTGAGCC ATTATTGCGCCACCAAAGCAGCCGTGATCAGCTATACCCAGAGTGCCGCACTGGCACTGGCACCG CATCGCATTAACGTGAATGGCATCGCCCCGGGTGTTGTGGATACCCCGATGTGGGAACAGGTGGA TGCCCTGTTTGCCCGCTACGAAAACCGCCCGCTGGGCGAGAAAAAACGTCTGGTGGGCGAAGCAG TGCCGCTGGGTCGTATGGGTGTGCCTGGCGATCTGACCGGTGCAGCCCTGTTTCTGGCCAGCGCAG ATGCCGACTATATTACCGCCCAGACCCTGAACGTTGACGGCGGTAATTGGATGAGCTGA
*Pd*PDH (GenBank accession no: WP_011751060)
ATGCGTCTGCAGGGCAAAACCGCGCTGATTACCGGAGCAGCTCGTGGTATTGGCCTGGAATTTGC CCGTGCCTATATTGCGGAAGGAGCGCGTGTGGCGCTGGCGGATATAAACGCCGATGCCGTGCGTG CGGCGGTGGAAAGCCTGGGCCCTCAAGCGGTCGCGGTGCAGATGGATGTCACCCGTCAGGATAGC ATTGATGCGGGCTTTGCAGAGGTGATTGGAACGTTTGGACATCTGGATATTCTGGTGAATAATGCG GCGCTGTTTACAGCAGCGCCTGTGGAAGAAGTGACACGTGCCGATTATGATCGTGTGATGGCAGT GAATATGACCGGTGCGTTTTTTTGTATGCAGGCAGCGGCAAAGCACATGATTGCGCGTGGCAAAG GCGGCAAGATCATTAACATGGCAAGCCAGGCGGGACGTCGTGGGGAACCGCTGGTGGCCGTGTA CTGCGCGAGCAAAGCGGCCGTGATTAGCATGACCCAGAGCGCAGGGCTGGGCCTGATTCGTCATG GCATCAACGTGAATGCAATCGCGCCAGGGGTGGTAGATGGGGAGCATTGGGATATGGTCGATGA ACATTTTGCACGTTTCGAAGGCCTGAAACCGGGCGAGAAGAAAAAACTGGTGGGTGCAGCGGTGC CGTTTGGCCGTATGGGCGTAGCCAGCGACCTGACCGGCATGGCGATTTTTCTGGCCACCGCGGAA GCGGAATATATCGTGGGCCAGACCTTTGGAGTTGACGGAGGGAATTGGCTGGCTTGA
*Ps*PDH (GenBank accession no: WP_005733884)
ATGAAACGTCTTGAAGGCAAATCAGCGTTAATTACCGGCAGCGCGCGTGGCATTGGCCGTGCGTT TGCCCAAGCGTATATTCAGGAAGGAGCCCGGGTGGCTATCGCGGATATTAACCTGCAGCGTGCGC AGGCGACCGCGAATGAACTGGGCCCGAATGCGTATGCGGTGAGCATGGATGTGACCGATCAGAC CAGCATTGATCAGGCGATTGCCGCGGTAGTGGCGAAAACCGGCAAATTGGACATCTTGATTAACA ACGCGGCACTGTTTGATCTGGCGCCGATTGTGGATATCACCCGTGATTCCTATGAACGTCTGTTTT CAATTAATGTGGCGGGCACCTTATTTACCTTACAGGCAGCGGCACGGCAGATGATTGCTCAGGGG CATGGCGGCAAAATCATCAATATGGCGAGCCAGGCGGGTCGTCGTGGCGAGGCGCTGGTGGCGGT GTACTGCGCGACCAAAGCGGCGGTCATCAGCTTAACCCAGAGCGCTGGGCTGGATCTGATTCGTC ATGGCATTAACGTAAATGCTATTGCTCCCGGTGTGGTGGATGGGGAACATTGGGATGGAGTGGAT GCGATGTTTGCGCGTTATGAAAATCGTCCGCTGGGTGAAAAAAAGAAACTGGTGGGCGAACAAGT GCCGTATGGCCGGATGGGCACCGCCGATGATCTGACAGGGATGGCGATCTTTCTGGCGTCGCCGG ATAGCGAATATGTGGTAGCGCAGACCTATAATGTCGATGGAGGCAACTGGATGAATTGA
*Ca*PDH (GenBank accession no: KGR09136)
ATGAGCAAAGAAACCACCAGCTACACCAATGCGAAACTGGGCCCGTTACCTACCAAAGCGGCGA CCATTCCGGACAATATTCTGGATGCGTTTAGCCTGAAAGGCAAGGTGGCCAGCGTTACCGGCAGC AGCGGTGGGATAGGTTGGGCGGTGGCGGAAGGATATGCGCAGGCGGGTGCAGATGTCGCGATTT GGTATAATAGCCATCCGGCGGATGATAAAGCGGAGTATTTGACCAAAACCTATGGCGTCAAAAGC AAAGCGTATAAGTGCAATGTGACCGATTTCCAGGATGTGGAAAAAGTGGTGAAACAGATTGAAA GCGATTTTGGCACCATCGATATTTTCGTAGCGAATGCAGGCGTGGCGTGGACCGAAGGCCCGGAA ATTGATGTCAAAGGTGTGGATAAATGGAATAAAGTAGTGGACGTGGATCTGAATAGCGTGTATTA

TTGTGCCCATGTGGTGGGGCCGATTTTCCGTAAAAAGGGCAAAGGCAGCTTCATCTTTACTGCCAG CATGAGCGCGAGCATTGTGAATGTGCCGCAACTGCAAGCGGCCTATAATGCGGCAAAAGCGGGA GTGAAGCATCTGTCAAAAAGCCTGAGCGTGGAATGGGCTCCGTTTGCGCGTGTGAACTCGGTGTC TCCGGGGTACATAGCGACCCATCTGAGCGAATTTGCGGATCCAGATGTGAAATCAAAATGGCTGC AACTGACCCCGTTAGGCCGTGAAGCTAAACCGCGGGAACTTGTGGGCGCGTATCTGTATCTGGCG AGCGATGCCGCGAGCTATACCACAGGTGCGGACTTGGCGGTTGATGGTGGATATACCGTAGTCTG A
*St*NOX (GenBank accession no: AIC24657)
ATGGATAAATTCATGAGCAAAATTGTGGTCGTGGGCGCGAATCATGCGGGCACCTATAGCATTAA TACGATTCTGGACAATTATGGGGACCAGAATGAAGTAGTGGTTTTCGATCAGAACAGCAATATTA GCTTTCTGGGCTGCGGCATGGCGCTGTGGATTGGCAATCAGATATCCGGTCCGGATGGCTTGTTTT ATGCGAATAAAGAAGTACTGGAATCTAAAGGTGCGAAGGTCTACATAAACAGCCCGGTAGAAAG CATTGATTTTGATGGAAAGACAGTGACCGCGCTGGTGGATGGCAAAGAACACGTGGAGTCCTACG ATAAACTGATTCTTGCGACGGGCTCCCAGCCCATTCTGCCGCCGATCGATGGCGCAGAAATCAAA GAGGGCAGCCGTACCTTTGAAGCGACCCTGGAAAACCTGCAGTTTGTGAAACTGTTTCAGAACGC TCAGGAGGTGATTGATAAGCTGAATGATAAAAGCCAGGACATTAAGCGTGTGGCGGTGGTGGGGG GCAGGTTATATTGGCGTGGAACTGGCAGAAGCATTCCAGCGTCATGGCAAGGAGGTCATACTTAT AGATGTGGTTGATACCTGCTTGGCGGGTTATTATGATCGGGATTTTACAGATCGTATGGCTAAAAA TCTGGAAGATCACGGGATTCAGTTAGCGTTTGGCGAAACCGTGAAAGCGGTGGAGGGAGAAACA AAAGTGGAACGTATTGTGACCGATAAGAACGCGTACGATGTGGATATGGTGGTGCTGGCCGTAGG CTTTCGTCCGAATACTGCTTTGGGCGCAGGCAAATTGGAAACCTTTCGTAATGGCGCGTATCTGGT GAATAAGAAACAGGAAACCAGCGTGAAGGATGTGTATGCAGTCGGGGATTGTGCGACCGTGTAC GACAATGCCCTGGATGATGTGAACTATATTGCGTTGGCAAGCAATGCGATTCGCAGCGGTATAGT CGCGGGTCATAATGCAGGAGGGGGGGATGTTGAATCAAATGGCGTGCAGGGCTCGAATGGCATCT CGATTTACGGCCTGAACATGGTCAGCACAGGCTTAACCGAAGAAAAAGCGAAGCGTTTTGGCTTT AATCCGGCGGTAGTGGAGAGCACCGATCTGCAAAAACCGCCGTTTATGAAAGATGAAAATGAAG ATGTGACGATTAAGATAGTCTATGACAAAGATACCCGTAAAGTCCTGGGGGCTCAGATGGTGAGC CTTATGGATATCAGCATGGGCATTCACATGTTTAGCCTGGCGATTCAGGAAGGCGTGACCATTGAT CGTCTGCAACTGCTGGATCTGTTTTTCCTGCCGCACTTCAATCAGCCGTTGAGTTATATCGCCAAG GCGGCGATTTCAGCCGAATGA

Fig. S4 SDS-PAGE analysis of recombinant biocatalysts.

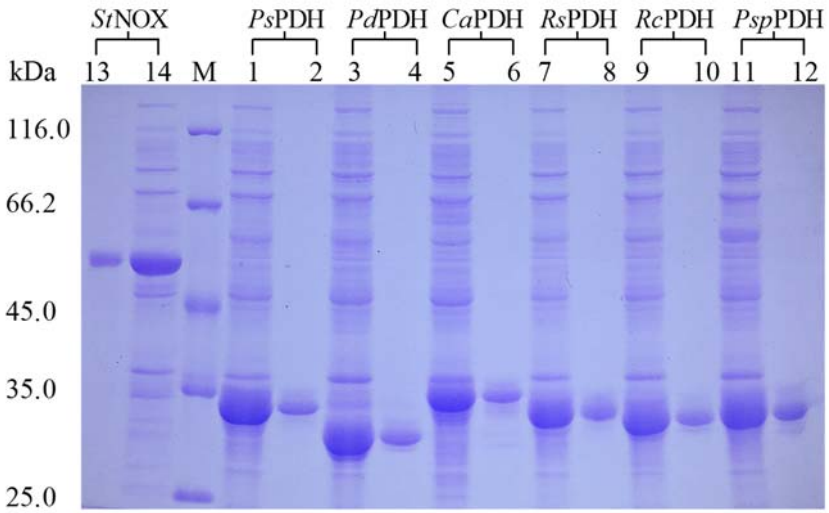

Lanes 1~14: supernatant and purified protein of *Ps*PDH (27.1 kDa), *Pd*PDH (26.7 kDa), *Ca*PDH (29.8 kDa), *Rs*PDH (27.0 kDa), *Rc*PDH (26.2 kDa), *Psp*SDH (27.5 kDa) and *St*NOX (50.1 kDa). M: Protein marker,116.0, 66.2, 45.0,35.0, 25.0 kDa (from top to bottom).

Fig. S5. Michaelis-Menton curve fit of *Pd*PDH with tested substrates (a~g) and *St*NOX with NADH (h).

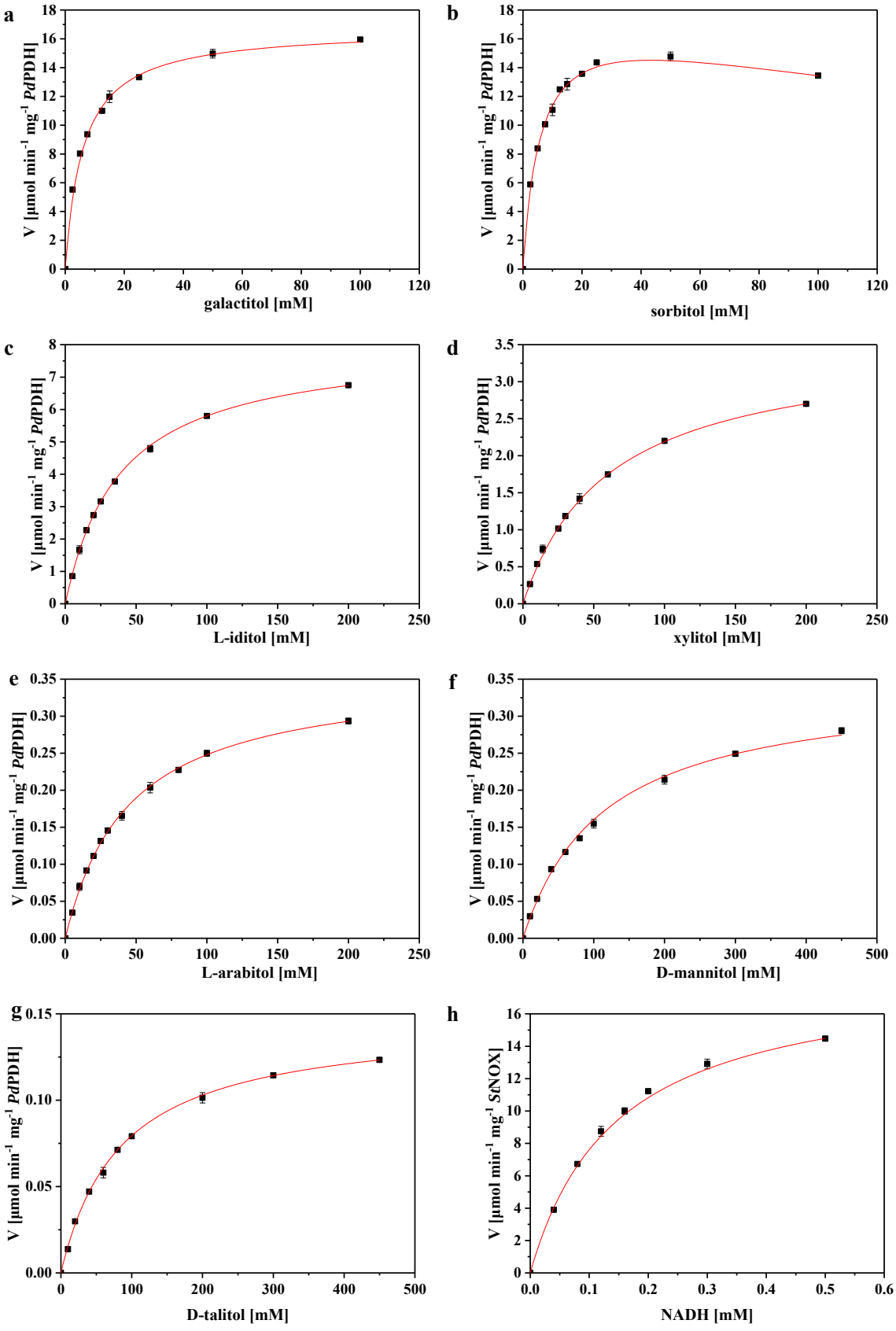

Fig. S6 A binding pose for **1a** in modelled *Pd*PDH complexed with NAD^+.

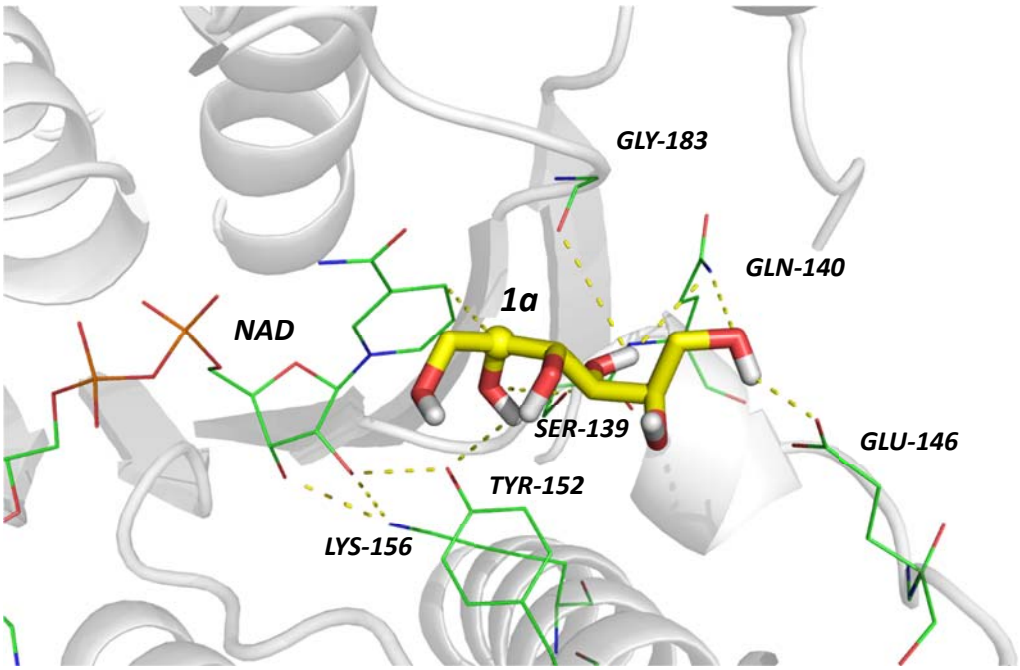

The key amino acid residues of the substrate-binding site are shown as Ser139, Tyr152, Lys156, Gln140, Glu146 and Gly183.

Fig. S7 Reduced product identification of *St*NOX.

Reduced product identification was performed by the 2,2-azino-bis (3-ethylbenzothiazoline-6-sulfonic acid) (ABTS) method as previously reported.[13] A *St*NOX assay mixture containing 0.2 mM NADH was incubated at 30 ºC until the A_{340} of the solution was lower than 0.01, indicating that almost all the NADH had been oxidized. The solution product (200 μL) was then combined with 50 μL of a solution containing ABTS (0.2 mg mL^{-1}) and 100 U mL^{-1} horseradish peroxidase. A control *St*NOX assay mixture containing 10 μM H_2O_2, but lacking NADH, was processed similar to those described above. Lanes 1~2: Control (Green: containing 10 μM H_2O_2) and Reduced product (Colorless: no H_2O_2 was detected).

Fig. S8 Multiple sequence alignment of *St*NOX to known NADH oxidases. Secondary structure elements of *Spyo*NOX (PDB ID: 2bc0) are indicated above the sequence with arrows for β-strands and cylinders for α-helices. Strictly conserved residues are highlighted. FAD- and NAD-binding sites and catalytic regions are marked in bold letters. Figure was drawn using ESPript.[14]

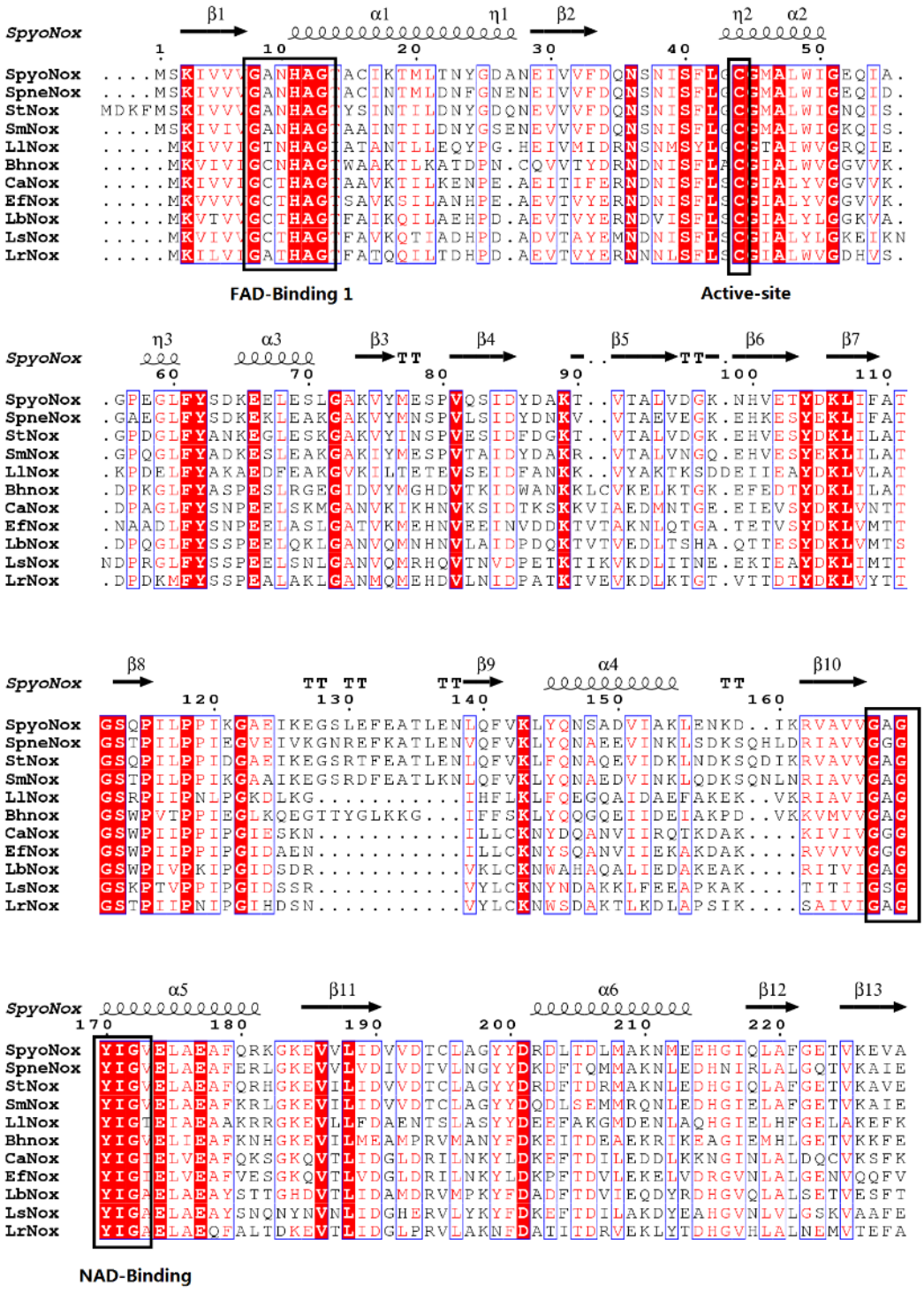

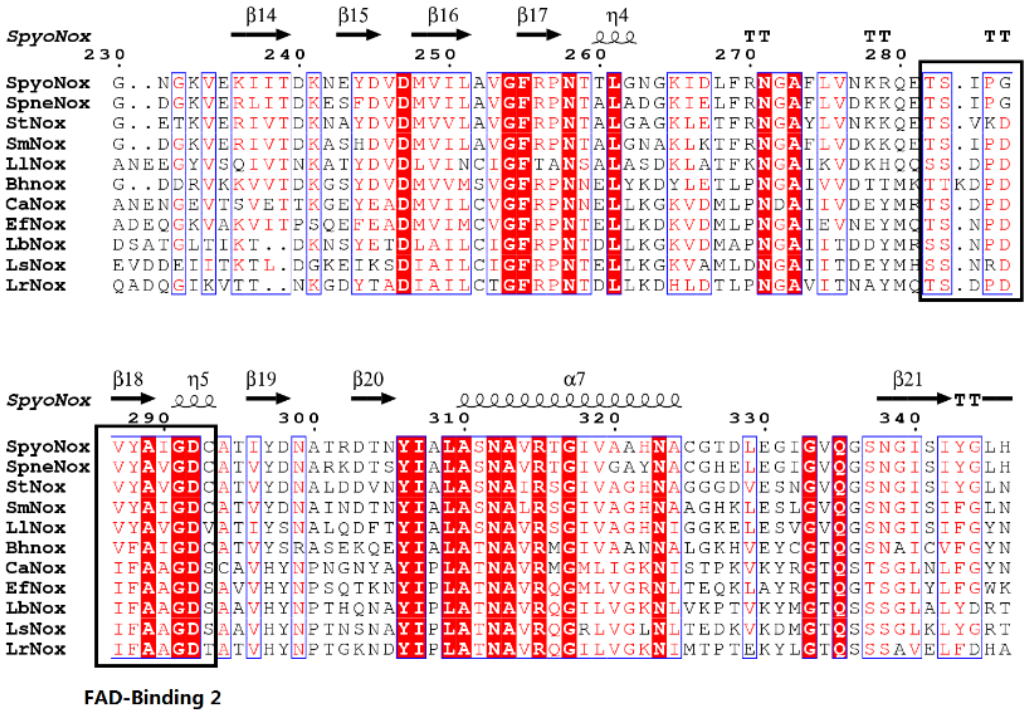

The amino acid sequence of *St*NOX has 76.79% identity with *Sm*NOX from *Streptococcus mutans*,[15] 75.54% identity with *Spyo*NOX from *Streptococcus pyogenes*,[16] 71.49% identity with *Spne*NOX from *Streptococcus pneumoniae*,[17] 50.32% identity with *Ll*NOX from *Lactococcus lactis*,[18] 47.20% identity with *Bh*NOX from *Brachyspira hyodysenteriae*,[19] 38.56% with *Lb*NOX from *Lactobacillus brevis*,[20] 39.53% with *Ef*NOX from *Enterococcus faecalis*,[21] 38.30% with *Ca*NOX from *Clostridium aminovalericum*,[22] 35.58% with *Lr*NOX from *Lactobacillus rhamnosus*,[23] and 34.60% with *Ls*NOX from *Lactobacillus sanfranciscensis*.[24] Alignment studies of the primary structure have demonstrated that *St*NOX shows homologies with the aligned sequences, containing a pivotal catalytic Cys44, one highly conserved sequence motif which is responsible for NAD binding (-GXGXXG-), and two FAD-binding domains (-GXXXXG-, and -TSXXDXXAXGD-).

Fig. S9 UV visible absorption spectra of purified *St*NOX

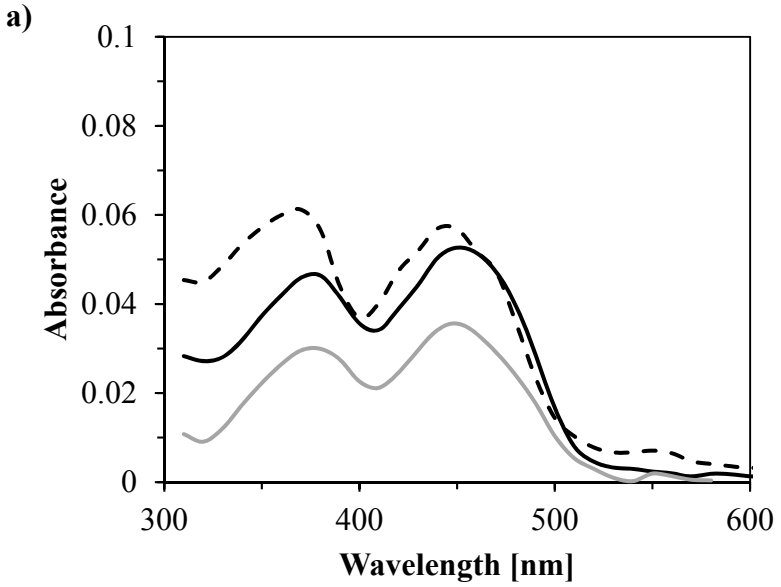

Purified NADH oxidase (200 µg) was dissolved in 200 µL 20 mM Tris-HCl buffer (pH 8.0) and scanned anaerobically at different wavelengths (310-600 nm) in a microplate reader (SpectraMax M5, Molecular Devices, Santa Clara, USA) at 30 °C. The absorption spectrum of *St*NOX indicates a typical flavin-containing protein, exhibiting the maximum absorbance at 379 and 450 nm (solid line).[22] Enzyme solution was then boiled for 10 min, cooled on ice, and centrifuged to remove denatured protein at 10,000×g for 15 min at 4°C. The yellow supernatant was confirmed to exhibit no oxidase activity and gave the same absorption spectrum as standard FAD (dashed line and gray line). Since it was released after treatment with hot water, the flavin coenzyme of the oxidase was non-covalently bound to the enzyme.

Fig. S10 Effect of exogenous flavin cofactor on the activities of recombinant *St*NOX.

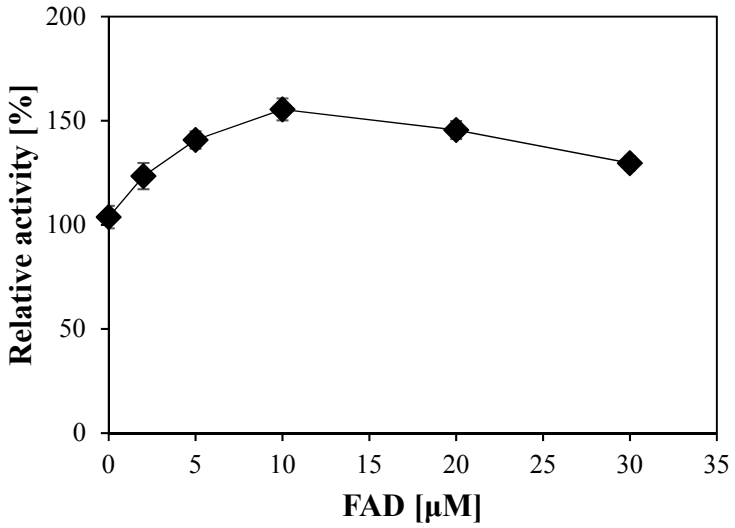

Purified enzymes (0.05 mg mL^{-1}) were incubated in Tris-HCl buffer (100 mM, pH 8.0) with different concentrations (from 0 to 30 µM) of FAD for 10 min. The activity was then determined under standard conditions. All measurements were performed in triplicate. Relative activity was shown as a percentage of the initial observed activity without flavin cofactor.

Fig. S11 Effect of pH and temperature on *Pd*PDH and *St*NOX activity.

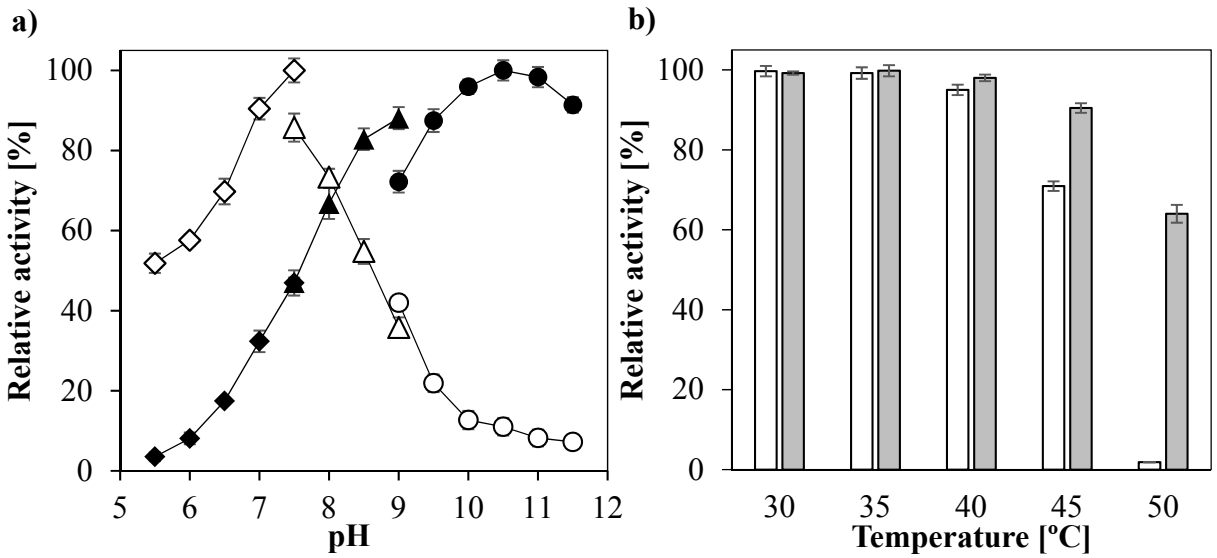

a) Optimum pH. Relative activity was shown as a percentage of the maximum activity for reducing NAD^+ by *Pd*PDH (Solid symbols) or oxidizing NADH by *St*NOX (opened symbols) under the experimental conditions. Enzymatic assay was performed at 30 ºC. Buffer of 100 mM sodium phosphate, Tris-HCl and Glycine-NaOH were shown as diamond, triangle and cycle, respectively. **b) Thermal stability.** Relative activity was shown as a percentage of the initial activity for reducing NAD^+ by *Pd*PDH (white columns) or oxidizing NADH by *St*NOX (grey columns) under the experimental conditions. Purified enzymes (0.5 mg mL^{-1}) were incubated in Tris-HCl buffer (100 mM, pH 8.0) for 2 h at various of temperatures (30, 35, 40, 45 or 50 ºC). The residual activity was then determined in Tris-HCl buffer (100 mM, pH 8.0) at 30 ºC. All measurements were performed in triplicate.

Fig. S12 HPLC analysis of the stability of NAD^+ under reaction condition.

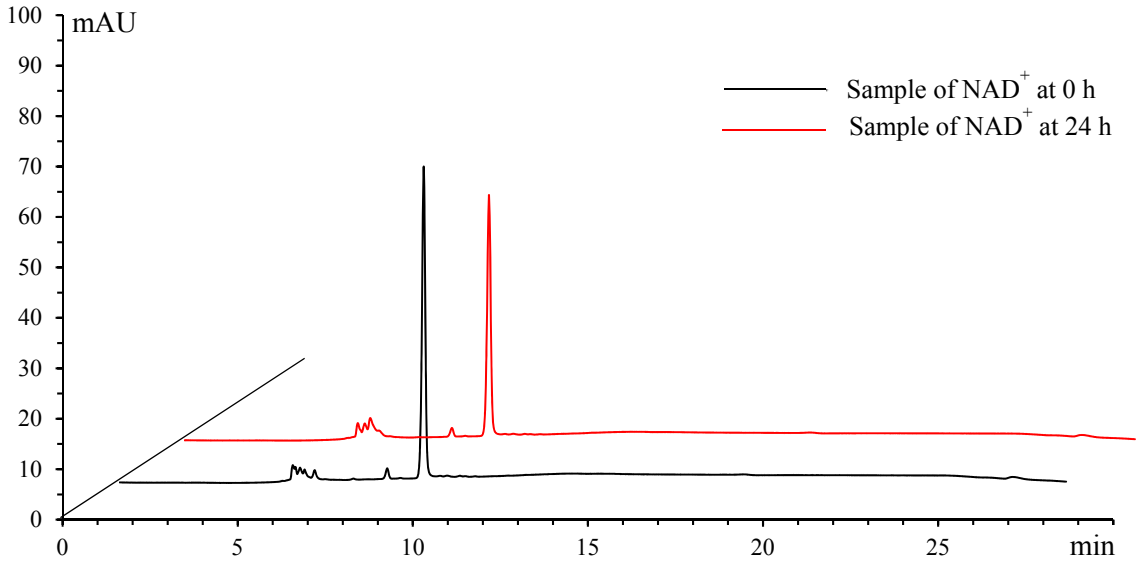

NAD^+ was diluted to the catalytic concentration of 0.2 mM in 10-mL 100 mM Tris-HCl buffer (pH 8.0). The dilute solution was then magnetically stirred at 30 °C at a constant speed of 1,000 rpm for 24 h. Quantification of NAD^+ was performed on a HPLC device (Ultimate 3000, Dionex, USA) equipped with the Sepax HP-C18 Column (SEPAX, USA), and detection at 260 nm. The mobile phase with a flow rate of 1 mL min^{-1} consisted of two eluents: Buffer A (5% acetonitrile and 20 mM KH_2PO_4 (5:95, v/v), pH 5) and Buffer B (water). The column temperature was maintained at 37 °C. After injecting the sample, the column was equilibrated with buffer B for 7 min, then B decreased to 0% while A increased to 100% at 7.5 min and held up to 20 min. The gradient was then returned to 100% B and 0% A at 21 min and the initial conditions were restored for the following 15 min. Retention time of NAD^+ was 8.67 min. The content of NAD^+ was obtained directly using calibration curves.

Table S5 Effect of metal ions and EDTA on the activity of *Pd*PDH and *St*NOX.

Metal ions [1 mM]	Relative activity [%][a]	
	*Pd*PDH	*St*NOX
Control	100.0	100.0
Na^{+}	101.7 ± 3.3	101.6 ± 0.4
Li^{+}	100.6 ± 5.1	102.2 ± 0.1
Co^{2+}	81.9 ± 2.7	99.0±0.1
Cu^{2+}	100.5 ± 0.2	0.0
Mg^{2+}	108.6 ± 3.9	99.1 ± 0.2
Mn^{2+}	106.1 ± 5.6	98.6 ± 0.3
Ni^{2+}	73.4 ± 5.4	89.8 ± 0.3
Zn^{2+}	68.2 ± 4.2	101.2 ± 0.2
Ca^{2+}	105.0 ± 0.2	71.8 ± 0.3
Fe^{2+}	88.0 ± 7.8	74.8 ± 0.2
Fe^{3+}	97.8 ± 2.6	70.2 ± 0.1
EDTA	101.6 ± 0.7	102.2 ± 0.1

Purified enzymes (0.5 mg mL^{-1}) were incubated in Tris-HCl buffer (100 mM, pH 8.0) for 20 min in the presence of the appropriate chemical at 30 ºC. After pre-incubation, the residual activity of the enzyme was measured under standard conditions. Relative activity was shown as a percentage of the control activity. All measurements were performed in triplicate.

Table S6 HPLC analysis conditions for polyols and its corresponding oxidation products.

Entry	Substrate	Product	Conversion determination	Ret. Time	$[\alpha]^D$
1	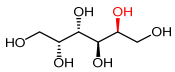 **1a**	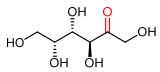 **2a**	Aminex HPX-87H, 5 mM H_2SO_4, 0.6 ml/min, col.: 65 °C	**1a**: 10.319 min **2a**: 9.633 min	-5.0°
2	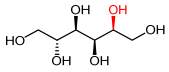 **1b**	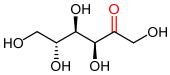 **2b**	Aminex HPX-87C, H_2O, 0.6 ml/min, col.: 85 °C	**1b**: 22.206 min **2b**: 14.380 min	-92.1°
3	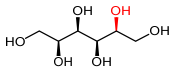 **1c**	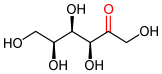 **2c**	Aminex HPX-87H, 5 mM H_2SO_4, 0.6 ml/min, col.: 65 °C	**1c**: 10.602 min **2c**: 9.483 min	-43.2°
4	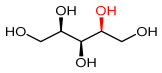 **1d**	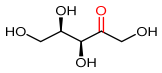 **2d**	Aminex HPX-87H, 5 mM H_2SO_4, 0.6 ml/min, col.: 65 °C	**1d**: 11.405 min **2d**: 10.434 min	-31.7°

Identification of the corresponding oxidation products of polyols.

Reaction conditions: **1a**, **1b**, **1c**, or **1d** (1.5 mmol), NAD^+ (1 μmol), *Pd*PDH (120 U), *St*NOX (480 U), and Tris-HCl buffer (100 mM pH 8.0, 10 mL), stirring under an oxygen atmosphere (O_2-balloon) in an Erlenmeyer flask (50 mL) at 1000 rpm and 30 °C. When conversion is complete, the reaction mixture was heated and centrifuged to remove the inactivated enzymes. After further purification by activated carbon and ion-exchange treatment, the oxidation product was analyzed by HPLC, and optical rotation ($[\alpha]^D$) was determined according to method described before.

HPLC analysis and spectra

1. HPLC profile for substrate 1a refined from XML and 2a standard

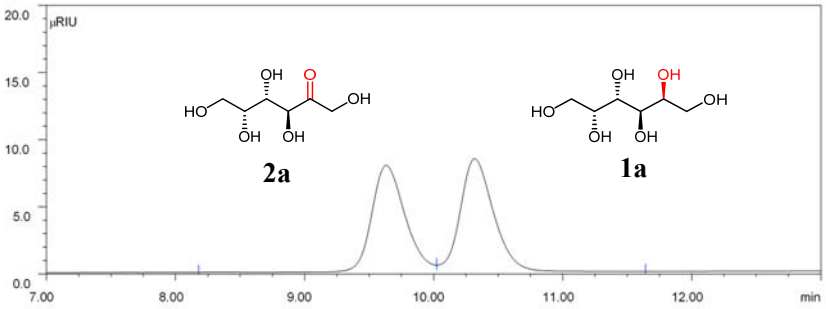

HPLC profile for bio-oxidation product of **1a** with *Pd*PDH

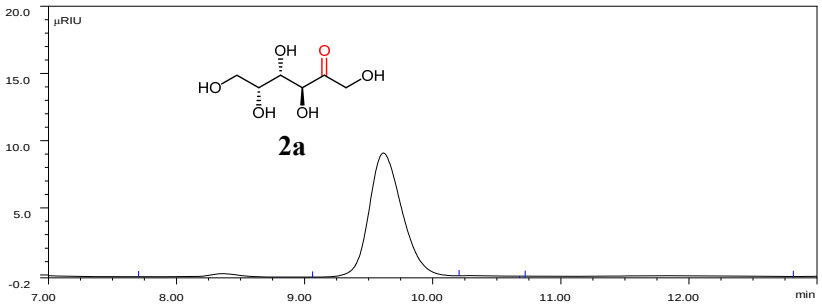

2. HPLC profile for 1b and 2b standards

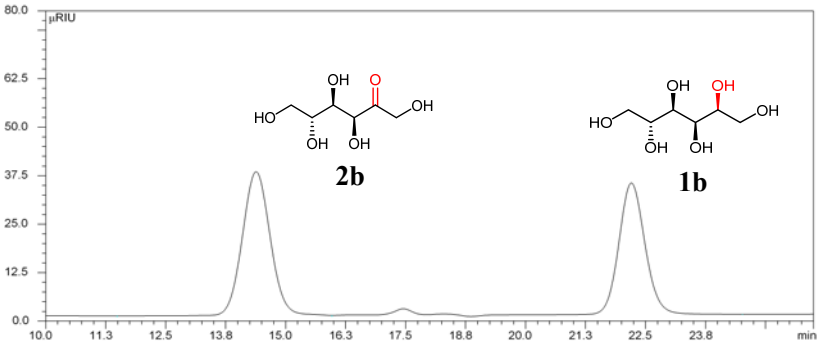

HPLC profile for bio-oxidation product of **1b** with *Pd*PDH

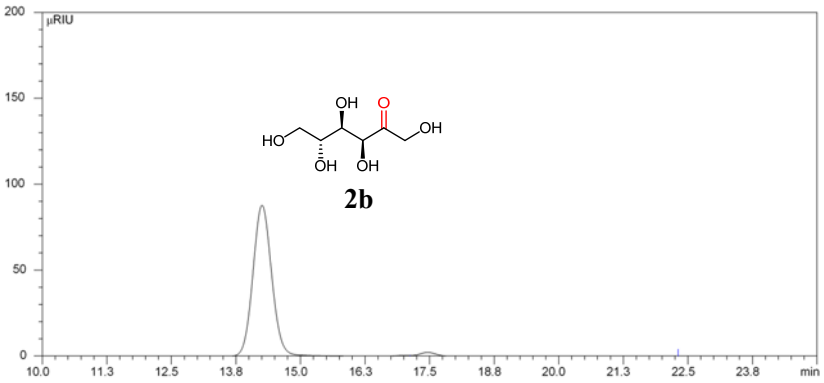

3. HPLC profile for 1c and 2c standards

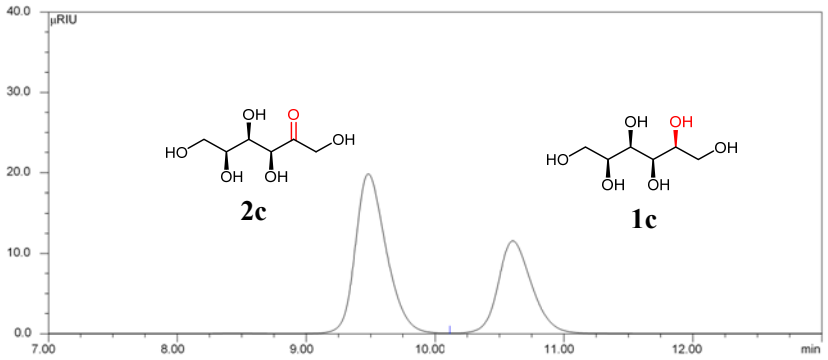

HPLC profile for bio-oxidation product of **1c** with *Pd*PDH

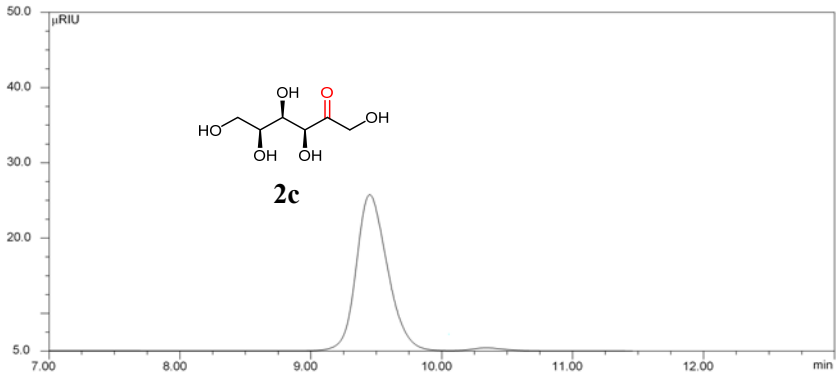

4. HPLC profile for 1d and 2d standards

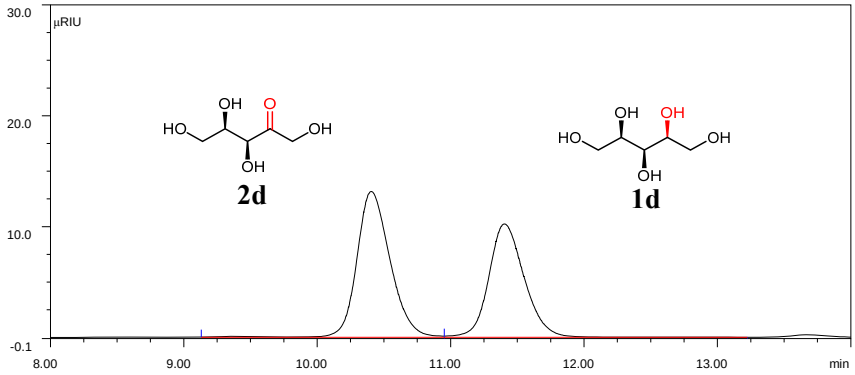

HPLC profile for bio-oxidation product of **1d** with *Pd*PDH

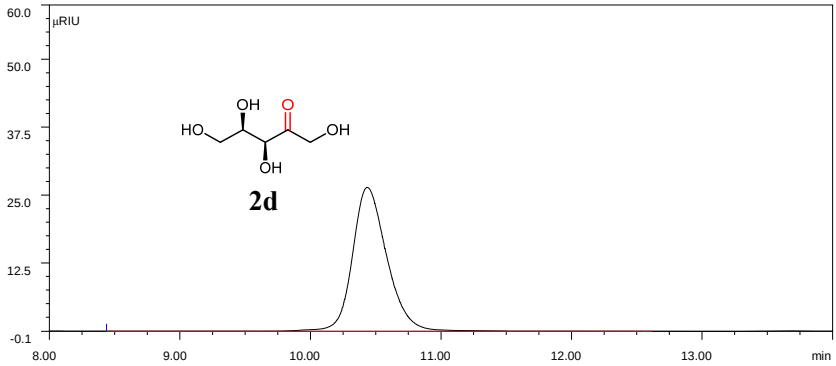

^{1}H NMR and ^{13}C NMR spectra

NMR profile for substrate **1a**[25]

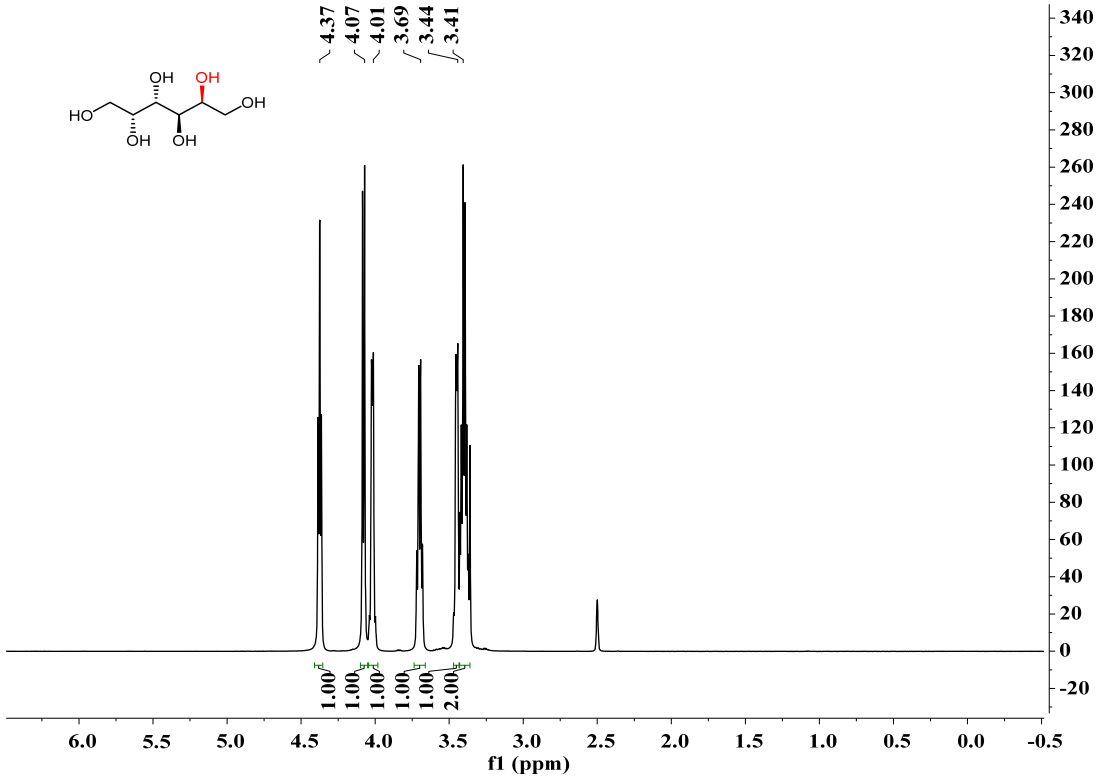

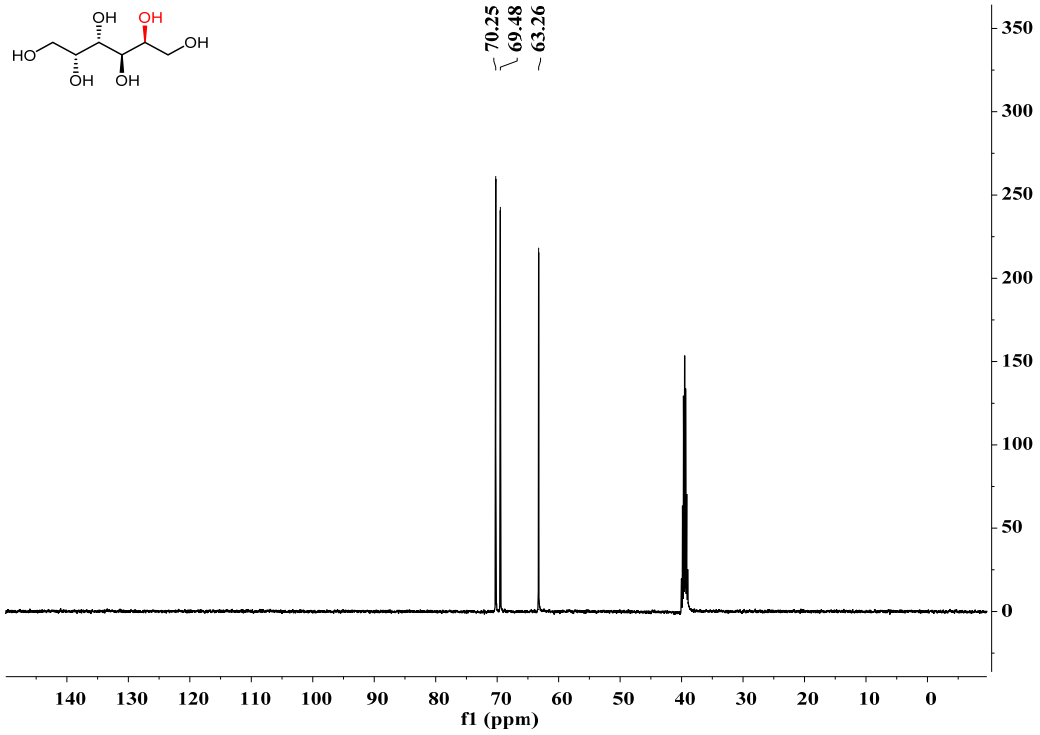

NMR profile for product **2a**[26]

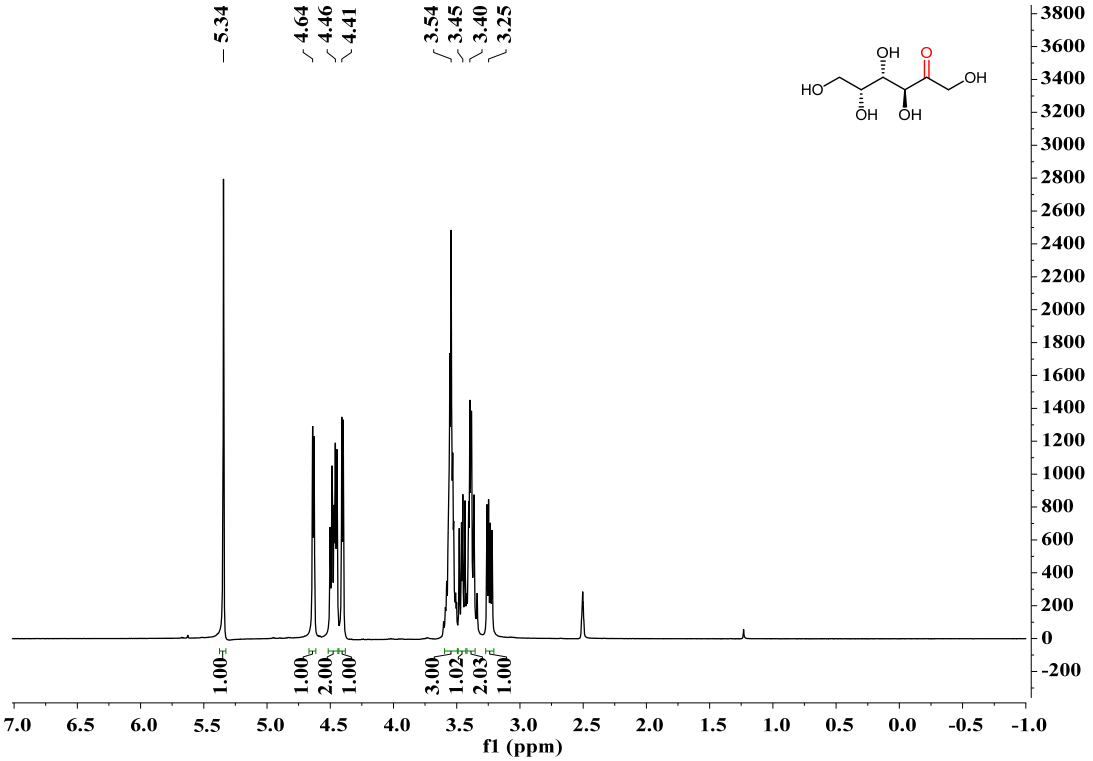

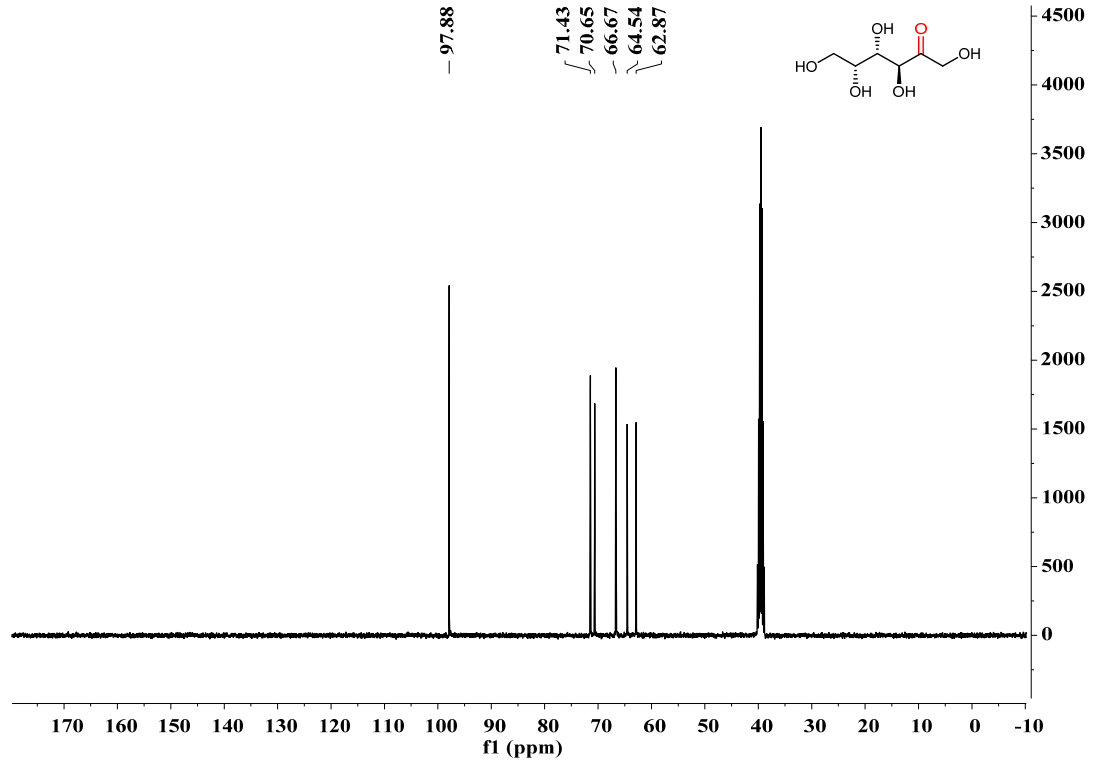

References

1. L. Wang, B. Zhao, B. Liu, B. Yu, C. Ma, F. Su, D. Hua, Q. Li, Y. Ma and P. Xu, *Bioresour. Technol.*, 2010, **101**, 7908-7915.

2. A. Wang, Y. Wang, T. Jiang, L. Li, C. Ma and P. Xu, *Appl. Microbiol. Biotechnol.*, 2010, **87**, 965-970.

3. H. Cheng, H. Wang, J. Lv, M. Jiang, S. Lin and Z. Deng, *Microb. Cell Fact.*, 2011, **10**, 43.

4. H. Cheng, B. Wang, J. Lv, M. Jiang, S. Lin and Z. Deng, *Microb. Cell Fact.*, 2011, **10**, 5.

5. Z. Liu, C. Ma, C. Gao and P. Xu, *Bioresour. Technol.*, 2012, **114**, 711-714.

6. Z. Li, H. Xiao, W. Jiang, Y. Jiang and S. Yang, *Appl. Biochem. Biotechnol.*, 2013, **171**, 555-568.

7. G. Zhang, Y. Lin, P. He, L. Li, Q. Wang and Y. Ma, *J. Ind. Microbiol. Biotechnol.*, 2014, **41**, 41-48.

8. H. Wang, J. Pan, J. Wang, N. Wang, J. Zhang, Q. Li, D. Wang and X. Zhou, *Biotechnol. Biotechnol. Equip.*, 2014, **28**, 1042-1049.

9. B. Tang, H. Xu, Z. Xu, C. Xu, Z. Xu, P. Lei, Y. Qiu, J. Liang and X. Feng, *Bioresour. Technol.*, 2015, **181**, 351-354.

10. T. Zhou and J. Zhong, *Bioresour. Technol.*, 2015, **175**, 160-166.

11. J. Guo, J. Li, Y. Chen, X. Guo and D. Xiao, *Appl. Biochem. Biotechnol.*, 2016, **180**, 717-727.

12. X. Liu, L. Lin, X. Xu, H. Zhang, L. Wu, P. Zhu, S. Li and H. Xu, *Carbohydr. Polym.*, 2018, **181**, 412-418.

13. D. E. Ward, C. J. Donnelly, M. E. Mullendore, J. van der Oost, W. M. de Vos and E. J Crane III, *Eur. J. Biochem.*, 2001, **268**, 5816-5823.

14. P. Gouet, X. Robert and E. Courcelle, *Nucleic Acids Res.*, 2003, **31**, 3320-3323.

15. B. Petschacher, N. Staunig, M. Müller, M. Schürmann, D. Mink, S. De Wildeman, K. Gruber and A. Glieder, *Comput. Struct. Biotechnol. J.*, 2014, **9**, e201402005.

16. H. Gao, M. K. Tiwari, Y. C. Kang and J. Lee, *Bioorg. Med. Chem. Lett.*, 2012, **22**, 1931-1935.

17. J. Yu, A. P. Bryant, A. Marra, M. A. Lonetto, K. A. Ingraham, A. F. Chalker, D. J. Holmes, D. Holden, M. Rosenberg and D. McDevitt, *Microbiology*, 2001, **147**, 431-438.

18. F. L. de Felipe and J. Hugenholtz, *Int. Dairy J.*, 2001, **11**, 37-44.

19. T. B. Stanton and R. Sellwood, *Anaerobe*, 1999, **5**, 539-546.

20. W. Hummel and B. Riebel, *Biotechnol. Lett.*, 2003, **25**, 51-54.

21. R. P. Ross and A. Claiborne, *J. Mol. Biol.*, 1992, **227**, 658-671.

22. S. Kawasaki, J. Ishikura, D. Chiba, T. Nishino and Y. Niimura, *Arch. Microbiol.*, 2004, **181**, 324-330.

23. Y. Zhang, M. K. Tiwari, H. Gao, S. S. Dhiman, M. Jeya and J. Lee, *Enzyme Microb. Technol.*, 2012, **50**, 255-262.

24. B. R. Riebel, P. R. Gibbs, W. B. Wellborn and A. S. Bommarius, *Adv. Synth. Catal.*, 2002, **344**, 1156-1168.

25. J. Vila, P. Mollinedo, Y. Flores and O. Sterner, *Rev. Boliv. Quim.*, 2008, **25**, 1-3

26. Y. Zhan, Z. Xu, S. Li, X. Liu, L. Xu, X. Feng and H. Xu, *J. Agric. Food Chem.*, 2014, **62**, 2412-2417.